JOURNAL OF MAGNETIC RESONANCE **125,** 188–192 (1997)
ARTICLE NO. MN961092

Pure-Phase Multidimensional NMR by Reference-Frequency Shift (RFS)

S. VENKATA RAMAN AND N. CHANDRAKUMAR

Laboratory of Chemical Physics, Central Leather Research Institute, Adayaru, Madras 600 020, Tamil Nadu, India

Received December 2, 1996

Multidimensional NMR (*1–3*), with isotope labeling (*4–8*) where appropriate, has revolutionized the capabilities of spectroscopy in investigations of molecular structure and dynamics. In these n-dimensional experiments, we deal with two or more time variables: one is the detection period t_n, during which the signal is actually sampled, while the others are virtual time variables $t_1, \ldots, t_{n-1}$, during which the system evolves undetected. Mixing or transfer periods could be sandwiched between any contiguous pair of these n time variables. Evolution during $t_1, \ldots, t_{n-1}$ modulates the signal acquired in the detection period. In the simplest case of two-dimensional spectroscopy, which involves just two time variables, evolution as a function of the virtual time variable t_1 modulates the phase or amplitude of the signal acquired during the detection period t_2. Issues in spectral acquisition, viz., spectral filtering, demodulation, and phasing, take on a special complexion when dealing with modulations in virtual time. We report in this Communication a simple novel approach to pure-phase multidimensional NMR with retention of quadrature information.

In general, the amplitude- or phase-modulated signal that arises in nD NMR results, on n-dimensional complex Fourier transformation, in a mixed-phase or phase-twisted lineshape (*9*) as we briefly recapitulate below (*cf.* Eq. [3]). A complex 2D signal has the general form

$$s(t_1, t_2) = u(t_1)\exp[-(\mathbf{i}\omega_e + T_{2e}^{-1})t_1]u(t_2) \times \exp[-(\mathbf{i}\omega_d + T_{2d}^{-1})t_2], \quad [1]$$

where

$$u(t) = 0, \quad t < 0$$
$$= 1, \quad t > 0.$$

Doing a complex 2D FT on Eq. [1], we have

$$S(\omega_1, \omega_2) = [T_{2e}^{-1} + \mathbf{i}(\omega_1 + \omega_e)]^{-1} \times [T_{2d}^{-1} + \mathbf{i}(\omega_2 + \omega_d)]^{-1}. \quad [2]$$

Rewriting Eq. [2] explicitly in terms of the absorptive and dispersive parts, we have the well-known mixed-phase lineshape

$$S(\omega_1, \omega_2) = [A(\omega_1) - \mathbf{i}D(\omega_1)] \times [A(\omega_2) - \mathbf{i}D(\omega_2)]$$
$$\equiv [A(\omega_1)A(\omega_2) - D(\omega_1)D(\omega_2)] - \mathbf{i}[A(\omega_1)D(\omega_2) + D(\omega_1)A(\omega_2)]. \quad [3a]$$

Here,

$$A(\omega_1) = T_{2e}^{-1}[T_{2e}^{-2} + (\omega_1 + \omega_e)^2]^{-1}$$
$$D(\omega_1) = (\omega_1 + \omega_e)[T_{2e}^{-2} + (\omega_1 + \omega_e)^2]^{-1}. \quad [3b]$$

Corresponding definitions hold for $A(\omega_2)$ and $D(\omega_2)$.

Similarly, an amplitude-modulated signal of the form

$$s(t_1, t_2) = u(t_1)\cos(\omega_e t_1)\exp(-t_1/T_{2e})u(t_2) \times \exp[-(\mathbf{i}\omega_d + T_{2d}^{-1})t_2] \quad [4]$$

results, on complex 2D Fourier transformation, in

$$S(\omega_1, \omega_2) = \frac{1}{2}\left\{\left(\frac{T_{2e}^{-1}}{T_{2e}^{-2} + (\omega_1 - \omega_e)^2} + \frac{T_{2e}^{-1}}{T_{2e}^{-2} + (\omega_1 + \omega_e)^2}\right) - \mathbf{i}\left(\frac{(\omega_1 - \omega_e)}{T_{2e}^{-2} + (\omega_1 - \omega_e)^2} + \frac{(\omega_1 + \omega_e)}{T_{2e}^{-2} + (\omega_1 + \omega_e)^2}\right)\right\} \times [T_{2d}^{-1} + \mathbf{i}(\omega_1 + \omega_d)]^{-1}. \quad [5]$$

Separating the absorptive and dispersive components, we have

$$S(\omega_1, \omega_2) = \frac{1}{2}\{A(\omega_1) + A(-\omega_1) - \mathbf{i}[D(\omega_1) + D(-\omega_1)]\} \times [A(\omega_2) - \mathbf{i}D(\omega_2)]$$

1090-7807/97 $25.00

$$\equiv \frac{1}{2}[A(\omega_1) + A(-\omega_1)]A(\omega_2) - [D(\omega_1) + D(-\omega_1)]D(\omega_2) - \frac{\mathbf{i}}{2}\{[A(\omega_1) + A(-\omega_1)]D(\omega_2) + [D(\omega_1) + D(-\omega_1)]A(\omega_2)\}. \quad [6]$$

This clearly corresponds to a pair of phase-twisted lines symmetric with respect to $\omega_1 = 0$. The magnitude-mode spectrum or power spectrum of such a data set would lead to broad lines, because of the contribution from the dispersive tails, resulting in loss of resolution.

A real FT with respect to t_1 and a complex FT with respect to t_2 of Eq. [4], on the other hand, results in

$$S(\omega_1, \omega_2) = \frac{1}{2}\left\{\frac{T_{2e}^{-1}}{T_{2e}^{-2} + (\omega_1 - \omega_e)^2} + \frac{T_{2e}^{-1}}{T_{2e}^{-2} + (\omega_1 + \omega_e)^2}\right\} \times [T_{2d}^{-1} + \mathbf{i}(\omega_2 + \omega_d)]^{-1}. \quad [7]$$

Separating Eq. [7] into absorptive and dispersive parts, we have

$$S(\omega_1, \omega_2) = \frac{1}{2}[A(\omega_1) + A(-\omega_1)] \times [A(\omega_2) - \mathbf{i}D(\omega_2)] \equiv \frac{1}{2}[A(\omega_1)A(\omega_2) + A(-\omega_1)A(\omega_2)] - \frac{\mathbf{i}}{2}[A(\omega_1)D(\omega_2) + A(-\omega_1)D(\omega_2)]. \quad [8]$$

From the real part of Eq. [8], it can be seen that the real (cosine) ω_1 transform of a signal that is amplitude modulated in t_1 results in a pure-phase spectrum, but is associated with a sign ambiguity of the frequencies in F_1. In order to obtain a pure-phase spectrum while retaining quadrature information in F_1, we must resort to special tricks such as the hypercomplex strategy (*10, 11*) or the TPPI procedure (*12–14*).

In this Communication, we draw attention to a simple alternative procedure for obtaining pure-phase multidimensional spectra by introducing an offset term in the evolution Hamiltonian. This is accomplished by *r*eference *f*requency shift (RFS) during the evolution period.

To set our work in perspective, we briefly summarize below the two standard strategies of pure-phase *n*D spectroscopy with retention of quadrature information. In the hypercomplex procedure of States *et al.* (*10*), a pair of experiments is performed, the two members of which differ in the n-quantum preparation pulse phases by $\pi/(2n)$. For an n-quantum coherence, this corresponds to a phase shift of $\pi/2$. Assuming that the amplitudes of the pathways from $+n$- and $-n$-quantum coherence are equal, we have for the two experiments

$$S_{\phi_P}(t_1, t_2) = u(t_1)\cos(\omega_e t_1)\exp(-t_1/T_{2e}) \times u(t_2)\exp[-(\mathbf{i}\omega_d + T_{2d}^{-1})t_2] \quad [9]$$

$$S_{\phi_P+\pi/2n}(t_1, t_2) = u(t_1)\sin(\omega_e t_1)\exp(-t_1/T_{2e}) \times u(t_2)\exp[-(\mathbf{i}\omega_d + T_{2d}^{-1})t_2]. \quad [10]$$

On performing a complex FT of Eqs. [9] and [10] with respect to t_2 and separating the absorptive and dispersive parts in ω_2, we have for the two experiments

$$S_{\phi_P}(t_1, \omega_2) = u(t_1)\cos(\omega_e t_1)\exp(-t_1/T_{2e})[A(\omega_2) - \mathbf{i}D(\omega_2)] \quad [11]$$

$$S_{\phi_P+\pi/2n}(t_1, \omega_2) = u(t_1)\sin(\omega_e t_1)\exp(-t_1/T_{2e})[A(\omega_2) - \mathbf{i}D(\omega_2)]. \quad [12]$$

Dropping the dispersion terms of Eqs. [11] and [12] and combining the real parts, we have

$$S(t_1, \omega_2) = \mathrm{Re}\{S_{\phi_P}(t_1, \omega_2)\} - \mathbf{i}\,\mathrm{Re}\{S_{\phi_P+\pi/2n}(t_1, \omega_2)\} = u(t_1)\exp[-(\mathbf{i}\omega_e + T_{2e}^{-1})t_1]A(\omega_2), \quad [13]$$

which on a complex FT with respect to t_1 followed by separation of absorptive and dispersive parts results in

$$S(\omega_1, \omega_2) = [A(\omega_1) - \mathbf{i}D(\omega_1)]A(\omega_2) = A(\omega_1)A(\omega_2) - \mathbf{i}D(\omega_1)A(\omega_2). \quad [14]$$

This is a four-quadrant pure-phase spectrum.

TPPI, on the other hand, is a procedure analogous to the Redfield trick in real time (*15*). For implementation in virtual time, the n-quantum preparation-pulse phases are incremented by $\pi/(2n)$ for each t_1-incremented experiment:

$$\Delta\phi_P = \frac{\pi}{2n\Delta t_1}\, t_1. \quad [15]$$

For an n-quantum coherence, this results in a phase shift of

$$n\Delta\phi_P = \frac{\pi}{2\Delta t_1}\, t_1. \quad [16]$$

This time-proportional phase shift corresponds to a frequency shift in F_1 given by

$$\Delta\nu = \frac{1}{2\pi}\frac{\pi}{2\Delta t_1} = \frac{\mathrm{SW}_1}{2}, \qquad [17]$$

where SW_1 is the spectral width in F_1. Thus, the TPPI procedure effectively shifts the frequency of the rotating frame to one end of the spectral window in F_1. Note also that coherences of order $\pm n$ are shifted in opposite directions by $\pm\mathrm{SW}_1/2$. The implication of course is that a real FT—which results in equally intense peaks at $\pm\omega_1$—is now nevertheless acceptable since only the spectral information in one of the two halves of F_1 is required, assuming equal amplitude of the $\pm n$-quantum coherence pathways.

It is clear from Eq. [17] that the TPPI procedure is equivalent to introducing an offset during the evolution time; this can be modeled by introducing an offset term $\Delta\omega I_z$ into the evolution Hamiltonian, under the action of which the same phase accumulation occurs during t_1 as given by Eq. [16]. On the basis of this model, we propose introducing the carrier offset during the evolution period directly in the frequency domain by phase-coherent switching of the reference frequency before the start of, and back at the end of, the evolution period. This is a straightforward alternative to TPPI, which involves cumbersome $4n$ step phase cycling in the time domain. Phase-coherent frequency switching was suggested earlier by Murdoch (*16*) for order separation of multiple-quantum coherences.

To obtain a pure-phase spectrum with quadrature information in F_1 by this procedure, we must shift the reference frequency phase coherently by half of the single-quantum spectral window before the start of the evolution period and switch it back to the middle of the spectral window at the end of the evolution period. Since this procedure is equivalent to the TPPI procedure, data processing can be done exactly the same way as is done for data sets obtained by the standard TPPI procedure. Note that the t_1 increment (''t_1 dwell'') should also be set as for the standard TPPI experiment.

The effect of offset on a general n-quantum coherence is given by

$$|i\rangle\langle j| \xrightarrow{\Delta\omega I_z\tau} \exp(-in\Delta\omega\tau)|i\rangle\langle j|. \qquad [18]$$

Hence a carrier frequency offset of $\mathrm{SW}_2/2$ actually results in a multiple-quantum frequency offset of $n(\mathrm{SW}_2/2)$, which is in fact half the F_1 spectral window for n-quantum coherence. Thus, to offset the carrier frequency by one-half of the *multiple quantum* spectral window, we shift the reference frequency phase coherently by half of the *single quantum* spectral window. The contrast with the TPPI procedure is to be noted in this respect, the latter protocol requiring both the preparation phase increments and the number of phase increments to be set in accordance with the order of coherence.

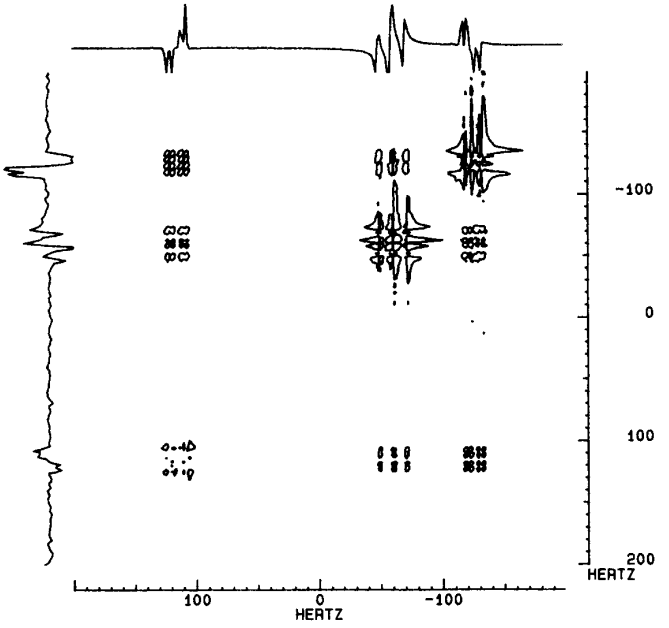

FIG. 1. Pure-phase proton COSY spectrum of 2,3-dibromopropionic acid in $CDCl_3$ obtained by the RFS procedure. Spectral width: 400 Hz in both dimensions; 512 t_1 increments, step size equal to the t_2 dwell. The reference frequency was offset by 200 Hz during the evolution time.

We demonstrate the application of the RFS procedure to obtain the pure-phase 2D COSY spectrum of 2,3-dibromopropionic acid in $CDCl_3$, as well as the double quantum and double quantum J spectra of 2-aminoethanol in D_2O. The experiments were all performed on a Bruker MSL 300 P spectrometer system. Fast phase coherent frequency switching was accomplished by modifying the strobe circuit (*17*) on the system's Fast/Slow I/O and Synthesizer Setting Board. The compiled version of the pulse program (filename extension **.PPG in DISMSL software) was also modified: for experiments without refocusing during the evolution period, which involve two frequency switchings, the frequency list strobe wait loop execution in the compiled program is disabled, resulting in a switching time of 3.65 μs (note that the switching time without these modifications is as long as 80 μs). For experiments with a refocusing pulse during the evolution period, involving four frequency switchings, the wait loop in the compiled pulse program is set to a single pass, resulting in a switching time of 4.65 μs.

It can be seen from Fig. 1 that as expected, the RFS-COSY diagonal peaks are in-phase dispersive while the cross peaks are in anti-phase absorption, as one has in a standard pure-phase COSY spectrum. The RFS-DQS (double-quantum spectrum) in Fig. 2 clearly displays anti-phase peaks in F_2 and in-phase multiplets in F_1. The spectrum obtained

(*18*) by the TPPI procedure is identical to Fig. 2; once again the same acquisition parameters and processing strategy were retained for the RFS experiment as for TPPI.

The double-quantum J spectrum of Fig. 3 demonstrates the effectiveness of the RFS strategy in obtaining pure-phase spectra with quadrature information when a refocusing pulse is applied in the middle of the evolution period. An identical spectrum results on performing the experiment by the TPPI procedure, with the same parameter settings. Note that SW_1 and SW_2 have no relation in such experiments. This experiment actually involves four frequency switchings (two for each half of the evolution period), unlike the two switchings of the earlier experiments. This can be understood on taking into account the effect of the refocusing pulse:

$$\exp(-\mathbf{i}\pi I_x)\Delta\omega I_z\exp(\mathbf{i}\pi I_x) = -\Delta\omega I_z. \qquad [19]$$

Clearly, the offset introduced by shifting the reference is also refocused along with chemical shifts and inhomogeneities. Taking into account the effect of the refocusing pulse in the middle of the evolution period, we modify the strategy for experiments involving a refocusing pulse during the evolution, in the following way: Instead of switching the reference frequency by $SW_1/(2n)$ for an n-quantum coherence, we switch the carrier by $SW_1/(2n)$ at the start of the first half of the evolution period and switch back to the middle of the window before issuing the refocusing pulse. The carrier is switched again by the same amount—but in the opposite sense—at the start of the second half of the evolution period and is switched back to the middle of the spectral window at the end of the evolution period. The net action generated during the evolution time under the offset Hamiltonian by this procedure is given by

$$\frac{SW_1}{2}\frac{t_1}{2}I_z + \exp(-\mathbf{i}\pi I_x)\left(-\frac{SW_1}{2}\right)\frac{t_1}{2}I_z\exp(\mathbf{i}\pi I_x) = \frac{SW_1}{2}t_1I_z. \qquad [20]$$

This expression has the form required to obtain quadrature information in F_1.

Note that RFS may be employed in real time to simulate ''quadrature detection'' using a single receiver channel; here one switches, after pulsing, from the middle of the spectral window to one end during the dead time and then commences data acquisition. The physical basis of RFS experiments may be simply understood by recalling that the output of the phase-sensitive NMR receiver is actually a function

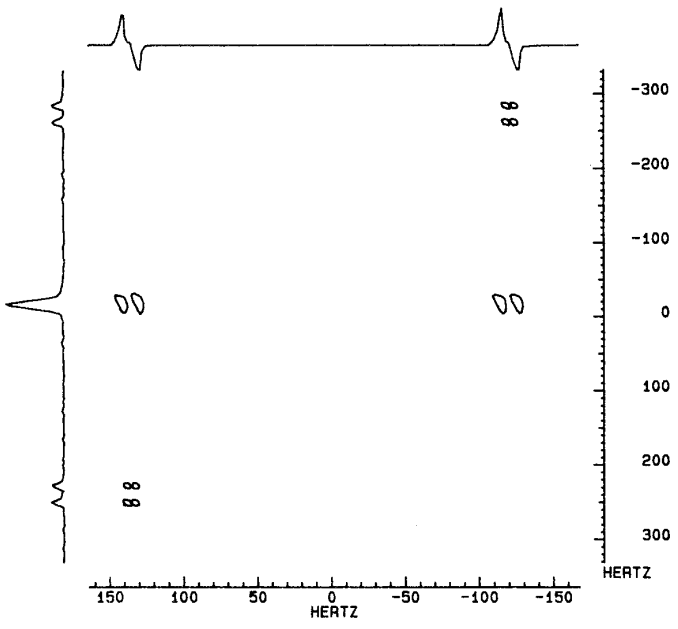

FIG. 2. Pure-phase proton double-quantum spectrum of 2-aminoethanol obtained by the RFS procedure. Spectral width: 360 Hz in F_2; 512 t_1 increments, step size equal to one-half the t_2 dwell. The reference frequency was offset by 180 Hz during the evolution time. F_1 projection shows the in-phase multiplets with one-group DQC exhibiting a splitting of $4J$; the plot also exhibits a row from the 2D data set, clearly displaying the anti-phase doublet structure resulting from reconversion of two-group DQC.

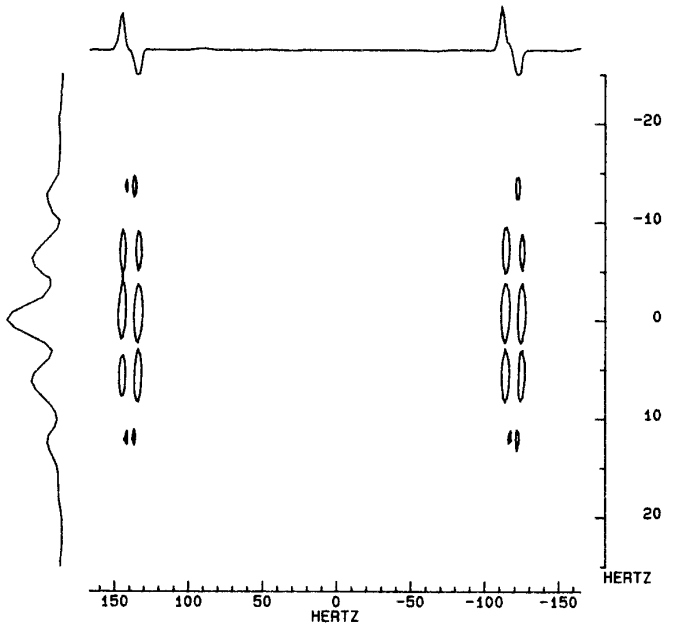

FIG. 3. Pure-phase proton double-quantum J spectrum of 2-aminoethanol obtained by the RFS procedure. Spectral width: 360 Hz in F_2; 128 t_1 increments, the spectral width in F_1 being 100 Hz (the plot does not display the two extreme quarters of the F_1 axis). The reference frequency was shifted by 25 Hz and −25 Hz before the first half and second half of the evolution period respectively. F_1 projection corresponds to the DQJ spectrum. The plot also exhibits a row from the 2D data set, clearly displaying the anti-phase doublet structure resulting from reconversion of two-group DQC.

of the phase difference between the signal and reference channels. Detailed implementation of the RFS strategy for application to a wide variety of *n*D NMR experiments is in progress in our laboratory.

ACKNOWLEDGMENT

S.V.R. is grateful to CSIR for a Senior Research Fellowship.

REFERENCES

1. J. Jeener, presented at Ampère International Summer School, Bosko Polje, Yugoslavia, 1971.
2. L. Müller, Anil Kumar, and R. R. Ernst, *J. Chem. Phys.* **63,** 5490 (1975).
3. W. P. Aue, E. Bartholdi, and R. R. Ernst, *J. Chem. Phys.* **64,** 2229 (1976).
4. D. M. LeMaster and F. M. Richards, *Biochemistry* **24,** 7263 (1985).
5. R. H. Griffey, A. G. Redfield, R. E. Loomis, and F. W. Dahlquist, *Biochemistry* **24,** 817 (1985).
6. P. H. Bolton, *J. Magn. Reson.* **62,** 143 (1985).
7. M. A. Weiss, A. G. Redfield, and R. H. Griffey, *Proc. Natl. Acad. Sci. USA* **83,** 1325 (1986).
8. G. Otting, H. Senn, G. Wagner, and K. Wüthrich, *J. Magn. Reson.* **70,** 500 (1986).
9. R. R. Ernst, G. Bodenhausen, and A. Wokaun, ''Principles of NMR in One and Two Dimensions,'' p. 31, Clarendon, Oxford, 1989.
10. D. J. States, R. A. Haberkorn, and D. J. Ruben, *J. Magn. Reson.* **48,** 286 (1982).
11. P. Bachmann, W. P. Aue, L. Müller, and R. R. Ernst, *J. Magn. Reson.* **28,** 29 (1977).
12. G. Drobny, A. Pines, S. Sinton, D. Weitekamp, and D. Wemmer, *Sympos. Faraday Soc.* **13,** 49 (1979).
13. G. Bodenhausen, R. L. Vold, and R. R. Vold, *J. Magn. Reson.* **37,** 93 (1980).
14. D. Marion and K. Wüthrich, *Biochem. Biophys. Res. Commun.* **113,** 967 (1983).
15. A. G. Redfield and S. D. Kunz, *J. Magn. Reson.* **19,** 250 (1975).
16. J. B. Murdoch, personal communication *cited in* D. Weitekamp, *Adv. Magn. Reson.* **11,** 111 (1983).
17. N. Chandrakumar and S. Sendhil Velan, *J. Magn. Reson. A* **104,** 363 (1993); S. Sendhil Velan, Ph.D. thesis, University of Madras, 1996.
18. N. Chandrakumar, ''Spin-1 NMR,'' NMR: Basic Principles and Progress, Vol. 34 (E. Fluck and H. Günther, Eds.), Springer-Verlag, Berlin, 1996; N. Chandrakumar, H.-E. Mons, D. Hüls, and H. Günther, *Magn. Reson. Chem.* **34,** 715 (1996).